Engineered Science
DOI: https://dx.doi.org/10.30919/es1351

Research of Methods to Improve the Accuracy of the Star Sensor for Global Navigation Satellite System Technology

Kamila Saurova,[1] Alexandr Shamro,[1] Kuanysh Alipbayev,[1] Saltanat Nysanbaeva,[1] Beibit Karibayev,[1, 5] Bakyt Khaniyev,[4, 5] Nursultan Uzbekov,[2, 3] Sabyrzhan Orynbassar,[2, 3] Zhanzira Geroyeva,[3] Adil Mukhamedgali[2] and Nursultan Meirambekuly[2, 3, 6,*]

Abstract

Star sensors are commonly used in satellite navigation systems to determine the orientation of spacecraft, which is crucial for accurate navigation and control. One of the key factors influencing the performance of a star sensor is its accuracy. However, this accuracy can be impacted by several factors, such as noise, stray light, optical aberrations, and errors during calibration. The article explores various methods to enhance the accuracy of star sensors and examines the image quality requirements necessary for Global Navigation Satellite System (GNSS) applications. Additionally, a software tool was chosen to support the analysis. Different design options for the star sensor's optical system were evaluated, including the parameters of the optical components of the lens and the characteristics of the optical radiation receiver, all of which play a role in determining the sensor's accuracy. The functionality of these components was also considered. Furthermore, the article investigates strategies for improving the sensor's accuracy. As a result of these investigations, a model of the optical system for the star sensor was developed. The Optics Software for Layout and Optimization (OSLO) software was used to model and analyze the star sensor's optical system in detail.

Keywords: Spacecraft; Star sensor; Optical system; Accuracy; Global navigation satellite system.
Received: 15 October 2024; Revised: 18 November 2024; Accepted: 23 November 2024.
Article type: Research article.

1. Introduction

The star sensor is an optical device that measures a spacecraft's orientation and the direction of stars in an image captured by the sensor's optical system relative to the spacecraft's coordinate system.[1-4] A star sensor with an accuracy of less than 1" is considered a high-precision device.[5] The development of ultra-precise star sensors is crucial for Earth observation and high-resolution astronomical studies, including the Global Navigation Satellite System (GNSS). Thanks to years of research, developers have gained a thorough understanding of star sensor errors, making it possible to further enhance the accuracy of these sensors.[6-12] Generally, all these requirements can be applied simultaneously. However, the combination of the requirement of accuracy with other requirements leads to their tightening. For example, an increase in the rotation speed of an aircraft can lead to a blurring of the image in the focal plane, which in turn can result in a decrease in the signal-to-noise ratio of the recorded stars and an increase in the error in orientation determination. Reducing the time, it takes to update information leads to a decrease in the duration of star exposure, which can lead to an increase in errors. High rotational speeds of the aircraft require either an increase in the field of view or a decrease in the duration of exposure.[13,14]

The main task set for the new generation of star sensors is to increase the accuracy of coordinate determination at a high polling rate. To achieve this, the following changes must be made to their design and operation:

[1] *Department of Space Engineering, Almaty University of Energy and Communications, Baitursynov street 126/1, Almaty, 050013, Kazakhstan*
[2] *Department of Science and Innovation, Kazakh-British Technical University, Almaty, 050010, Kazakhstan*
[3] *Center of Space Technologies, Al-Farabi Kazakh National University, Al-Farabi ave., Almaty, 050040, Kazakhstan*
[4] *Institute of Experimental and Theoretical Physics, Al-Farabi Kazakh National University, Al-Farabi ave., Almaty, 050040, Kazakhstan*
[5] *Department of Physics and Technology, Al-Farabi Kazakh National University, Al-Farabi ave., Almaty, 050040, Kazakhstan*
[6] *Ecology Research Institute, Khoja Akhmet Yassawi International Kazakh-Turkish University, Turkistan, 161200, Kazakhstan*
**Email:* Nursultan.Meirambekuly@kaznu.edu.kz (N. Meirambekuly)

- Reduce the angular size of pixels by using longer focal lengths, which results in smaller fields of view and the need to observe fainter stars (since brighter stars may not be visible in a narrower field);
- Measure the positions of the stars' centers on a charge-coupled device (CCD) matrix with an accuracy better than 0.1 pixels.[15]

There are several factors that can affect the accuracy of the star sensor, and one of the most significant is noise. Noise can originate from the camera sensor, electronic components, or processing algorithms. Stray light is another potential factor that can impact the accuracy of the star sensors. Stray light refers to light that enters the camera from other sources besides stars, such as the sun, moon, or Earth's atmosphere. Calibration errors are another significant source of inaccuracy in the star sensor. These errors can be caused by poor lighting conditions, such as fogging of the camera, filter wheel, or processor. The optical system of the star sensor needs to provide the required size of a star on the sensor detector and the required number of stars in the frame in order to accurately determine the angular position of the target using software.

Various researchers have investigated approaches for calibrating and validating the accuracy of the star sensors.[16-19] Xiaoyan *et al*. proposed a new star sensor optical machining precision alignment method, simulation-aided optical alignment, to improve the assembly precision of imaging components and solve practical engineering problems.[1] Sun *et al*. reported on a new and robust accuracy measurement method for a star tracker based on direct astronomical observation, which utilizes real navigation stars as observation targets, which makes the measurement results more authoritative and authentic.[20] Wang *et al*. designed a star sensor based on the principle of the field focal length (FFL), which can simultaneously enhance the field of view (FOV) and the single-star measurement accuracy.[21]

High-precision star sensors currently use a mechanical fitting method to assemble and adjust imaging components. The first step is to measure the pasting error between the detector chip and its mounting flange and then to compensate for the pasting error of the chip by repairing and replacing the focusing ring. The mechanical mounting surface of an optical lens mounting flange is then selected as the reference for mounting and adjusting the detector components. Finally, a focusing test is performed on the focusing ring that is compensated by the coping. According to this approach, the accuracy of the assembly of imaging components ranges from three to five angular components. This means that the assembly accuracy of such components is high and can meet the accuracy requirements of high-precision star sensors. The coping efficiency is low despite a high rejection rate, which makes it quite challenging to repair and replace the focusing ring.

There are two main methods for calculating the accuracy of star sensors: the theoretical calculation formula and the Monte Carlo algorithm. However, these are only representations of factors that partly influence attitude accuracy. As such, they cannot estimate star sensor accuracy in real time. Also, it is difficult to measure the real accuracy completely in a laboratory or in orbit. Therefore, it is necessary to develop a suitable method for measuring accuracy that is easy to use and implement and can meet high accuracy requirements.[22]

In this paper, a software product was selected to improve the accuracy of the star sensor, including the parameters of the optical components of the star sensor lens and the parameters of the optical radiation receiver, which affect the performance and parameters of these devices.

2. Experimental section

The star sensor's optical system must ensure the required size of the star on the detector of the star sensor and the required number of stars in the frame of the star sensor for accurate determination of its angular position with the help of a software. Thus, the software of the star sensor forms the main requirement for its optical system.

Considering all these requirements and factors, we took the following criteria into account while developing the optical system for our experimental model of the star sensor:
- The maximum stellar magnitude is 5.5, refresh rate – 2 Hz, weight – 1.5 kg;
- The full field of view should be at least 2/0 degrees in order to ensure the presence of at least three stars in the frame of the star with a brightness of at least 5.5;
- The minimum angle between the optical axis of the star and the Sun, ensuring the functional characteristics of the device, is not more than 40 degrees;
- The accuracy of determining the orientation around the optical axis is 60 arc seconds,
- The point spread function (PSF) was chosen so that the spot diameter of at least 85% of the energy covers about 10 square pixels. This allows the position of the center of mass of the star to be determined with sub-pixel accuracy.

In this paper two types of seven-lens optical systems that have spherical surfaces and diaphragms placed on the seventh lens for the star sensor were considered (OS1 and OS2) and the changes in their quality characteristics were investigated (Figs. 1 and 2). The best results were achieved with the seven-lens optical system that featured spherical surfaces and a diaphragm placed on the seventh lens.

Although this system meets the requirements for star sensors, it has several drawbacks. Since the entrance pupil is positioned on the 7th surface, the dimensions of the front lenses are larger than those of the entrance pupil, leading to increased lens size and, consequently, greater mass. To address this issue, the optical system was optimized by relocating the entrance pupil to the front surface (Fig. 2).

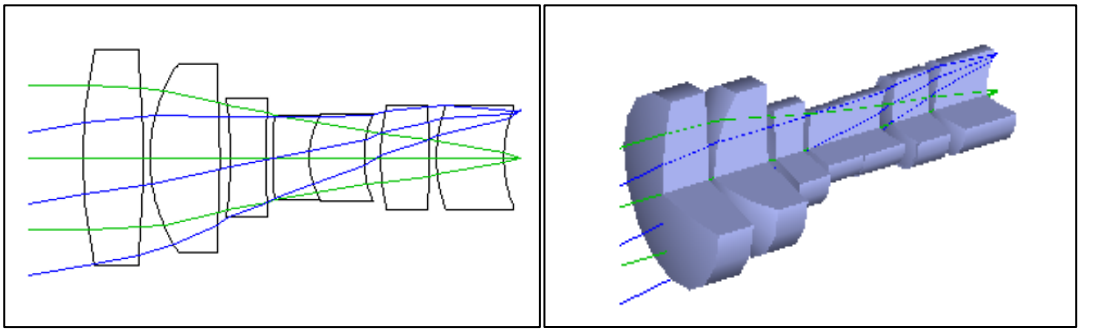

(A) (B)

Fig. 1: 2D (A) and 3D (B) models of the OS1 optical system of the star sensor.

Table 1. The geometric parameters of the OS2 optical system.

	Lens 1, ULTRAN20	Lens 2, N-SK11	Lens 3, FS	Lens 4, N-BASF2	Lens 5, N-SK11	Lens 6, N-SK16	Lens 7, SSK51
Radius of curvature of the surface 1, mm	65.154	24.23	-73,73	84.97	11.5	30.82	19.8
Radius of curvature of the surface 2, mm	-177.62	-152.33	105.3	11.5	15.67	-82.2	17.2
Thickness, mm	8.3	9.7	5	5	7.67	6.78	9.34
Distance between lenses n – n+1, where n = 1, mm.	1	1.45	1	0	2.29	1	-

The geometric parameters of the OS2 optical system are shown in Table 1.

The characteristics of the image produced by the seven-lens optical systems meet the requirements for a star image in the focal plane. Another advantage of this system is the wide range of options for glass used in the production of lenses.

3. Results and discussion

The accuracy of determining the position of a star is a crucial parameter of the star sensor, and it is limited by the aberrations of the optical system. Position measurement error is a significant source of error that needs to be minimized when designing the star sensor. The errors in the positions of the stars caused by aberrations are calculated in the optical system of the star sensor. Fig. 3 shows some of the resulting aberrations in the OS1 and OS2 optical systems. It can be seen that after optimization, the ray aberrations decreased by half. Figures 4 and 5 show the comparisons between other various types of aberrations in the OS1 and OS2 optical systems, such as astigmatism, longitudinal spherical aberration, chromatic focal shift, distortion, and lateral color aberration in the field 10° off-axis. Spherical aberration can be defined as the variation of focus with aperture. This occurs when the wavefront fails to conform to a sphere, resulting in incident light rays not focusing at the same point. Astigmatism occurs as a result of the tangential and sagittal images not focusing on the same plane. It is caused by a change of magnification with the field angle, shifting the Gaussian image point away from its ideal position. From the figure, it can be seen that both optical systems exhibit a negative distortion. However, for the optimized optical system, this distortion is reduced by 2 times.

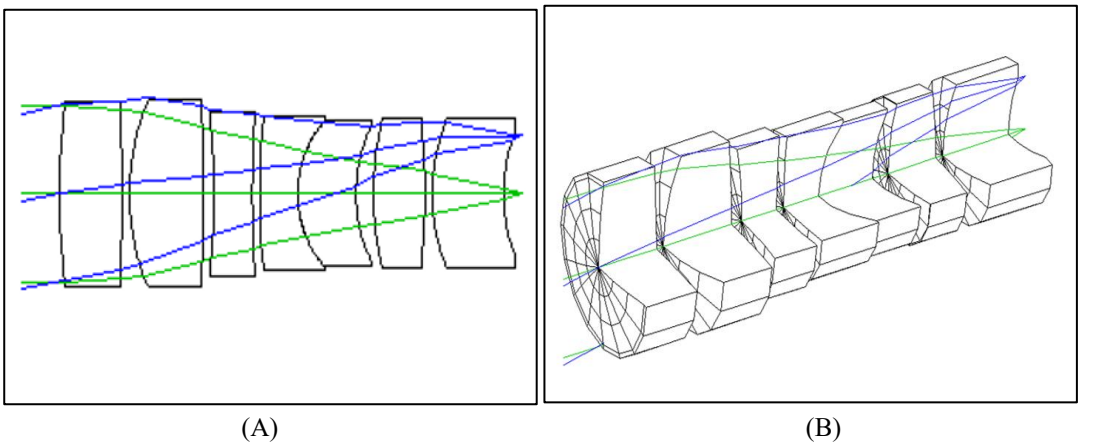

(A) (B)

Fig. 2: 2D (A) and 3D (B) models of the OS2 optimized optical system of the star sensor (λ_{green} = 0.588 μm, λ_{blue} = 0.486 μm).

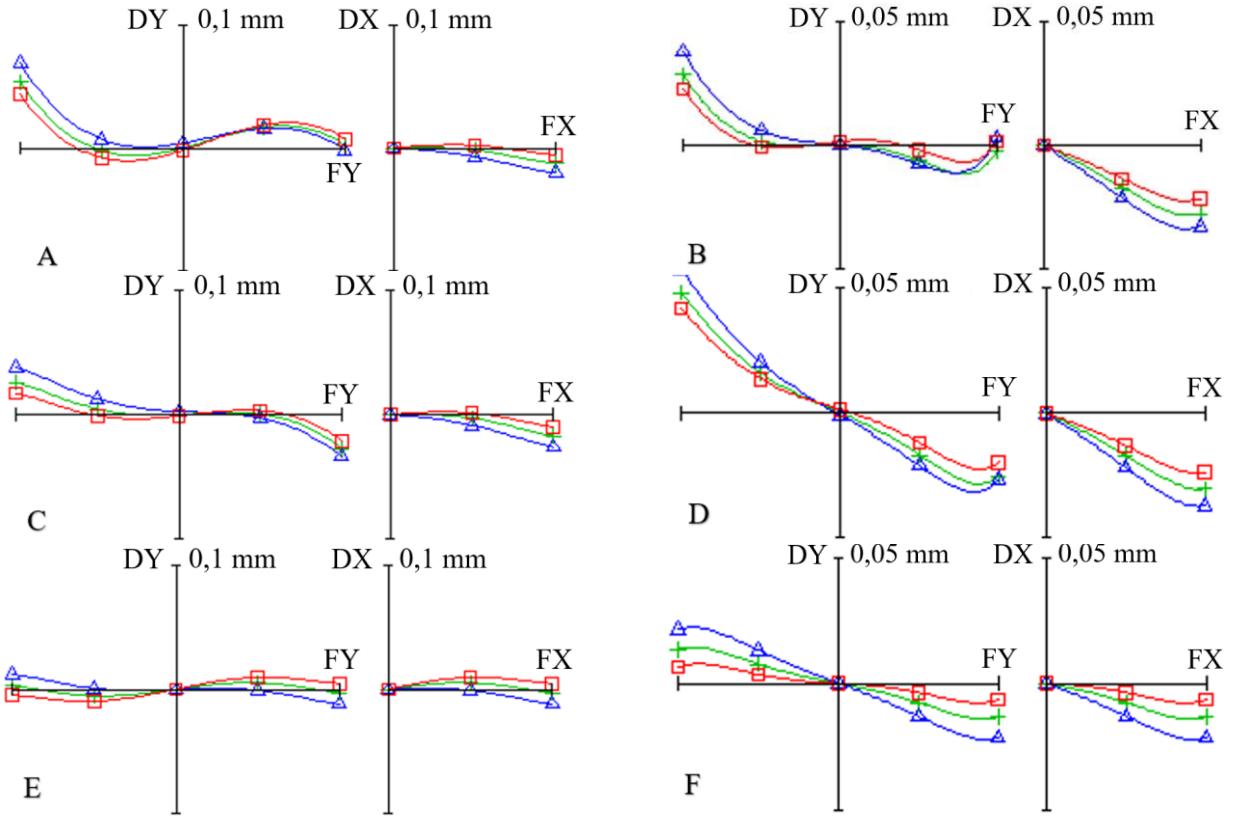

Fig. 3: Ray aberration curves of the OS1 (A, C, E) and OS2 (B, D, F) optical systems at arbitrary focuses plotted within 10 μm maximum scale in the field center (A, B), 7° (C, D) and 10° (E, F) off-axis, where $\lambda_{green\ (+)} = 0.588$ μm, $\lambda_{blue(\Delta)} = 0.486$ μm, $\lambda_{red(\square)} = 0.656$ μm, where DY – transverse ray aberration in the tangential section, DX – transverse ray aberration in the orthogonal section, FX and FY – heights in the pupil.

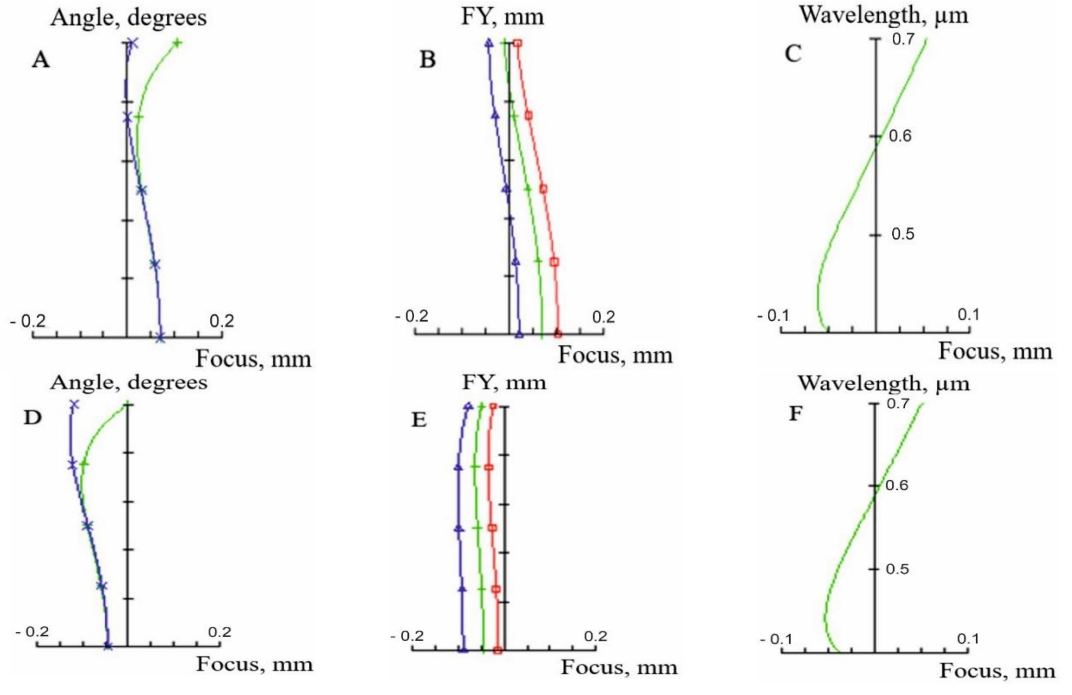

Fig. 4: Astigmatism (A, D), longitudinal spherical aberration (B, E), and chromatic focal shift (C, F) curves in the OS1 (A, B, C) and OS2 (D, E, F) optical systems in the field 10° off-axis. The astigmatism curves give the variation of paraxial focus across the field for the tangential section (green color curve) and the sagittal section (blue color curve). The longitudinal spherical aberration gives the movement of the focal point along the axis for different radii in the pupil, for the axial image point only, corresponding to the three wavelengths: $\lambda_{green\ (+)} = 0.588$ μm, $\lambda_{blue(\Delta)} = 0.486$ μm, $\lambda_{red(\square)} = 0.656$ μm. The curves for chromatic focal shift represent the axial beam paraxial longtitudal focal variation with wavelength over the range 0.4-0.7 μm.

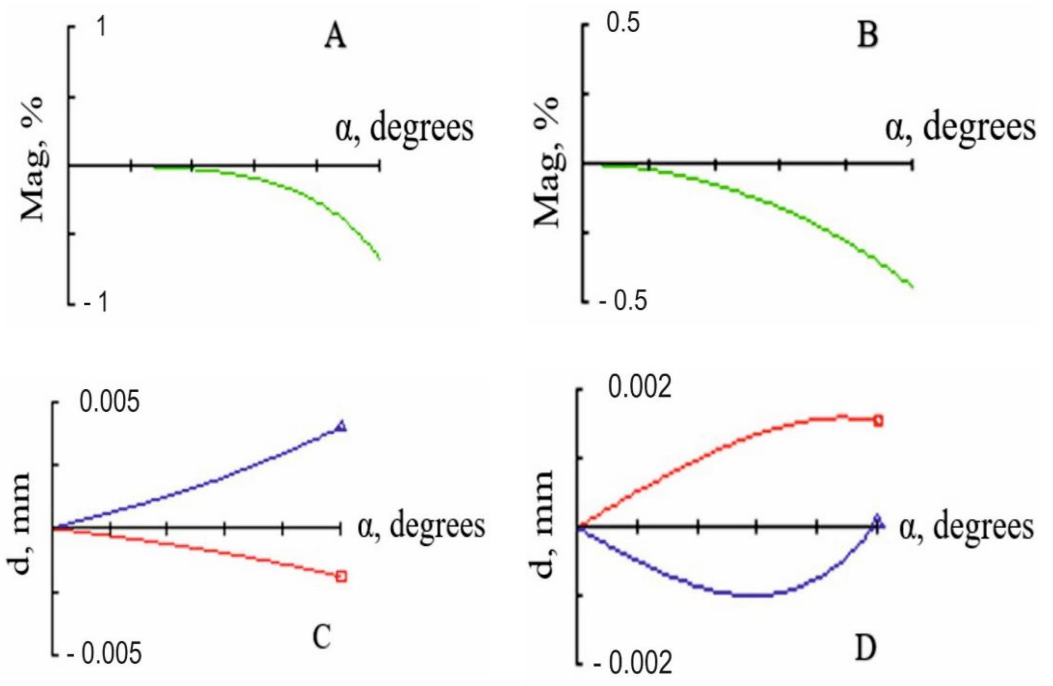

Fig. 5: Distortion (A, B) and lateral color aberration (C, D) curves in the OS1 (A, B, C) and OS2 (D, E, F) optical systems in the field 10° off-axis, where $\lambda_{green\ (+)}$ = 0.588 μm, $\lambda_{blue(\Delta)}$ = 0.486 μm, $\lambda_{red(\square)}$ = 0.656 μm. The curve for distortion shows the departure from the paraxial magnification as a function of field height. The curve for lateral color shows the difference between the heights of the red and green rays, and between the blue and green rays, as a function of field height.

Wavefront measurement is, by far, the most comprehensive way to assess the quality of the optical system. It is also correct to describe the resolution by the image shape of a distant luminous point, the PSF. Fig. 6 shows the resulting wavefront analysis of the OS1 and OS2 optical systems. Wavefront measurement is the most comprehensive way to assess the quality of an optical system. Indeed, the single wavefront measurement provides direct access to the aberrations of the lens of interest, as well as to the measurement of the MTF in all directions. The results indicate that the star position errors, caused by aberrations, are significant for high-precision star sensors, such as those that require arcsecond accuracy. After compensation is implemented, the star position errors decrease accordingly from their original values.

Computation of wavefront aberrations is a fundamental step in the assessment of the efficiency of optical systems especially in star sensors or any delicate instruments. It provides understanding the way how the optical system deviates light passing through the lens that can influence directly the image and the sensor accuracy. When performing wavefront analysis, two key metrics are often used to assess the quality of the optical system: root mean square (RMS) error and peak-to-valley (P-V) error**.** The RMS error measures the average deviation of the wavefront from the ideal (perfect) wavefront over the entire optical field. The P-V error measures the maximum deviation between the highest and lowest points of the wavefront from the ideal (perfect) wavefront. For star sensor systems**,** wavefront analysis is crucial in assessing how well the optical system can capture precise star images.

The optical system not only meets the specific requirements of diffuse spot and centralized energy distribution but also has a large aperture, low distortion, low color deviation, and insensitivity to defocus. The optical characteristics of the star sensor are quantitatively measured by the modulation transfer function (MTF) analyzer. 85% of the scattering spot energy for each field of view is concentrated in a circle with a diameter of 20 μm. The analysis of the PSF is shown in Fig. 7. To ensure the highest possible performance of the star sensor, the requirements for the lens PSF are based on the need to simultaneously ensure the detection of the star, the identification of its brightness and the determination of its angular position with maximum accuracy.

The PSF is a critical tool in optical system design and performance evaluation. It describes how a point source of light (like a star or laser) is spread out in the image due to imperfections in the optical system. The PSF is an essential measure of an optical system's ability to focus light and the sharpness of the resulting image. A smaller PSF with more energy concentrated in the central peak indicates better system performance and sharper, more accurate images. From Fig. 7, it can be seen that for OS2, the peaks are lower than those of OS1. For applications such as star sensors, a tight, concentrated PSF leads to higher accuracy in star position measurement and better overall system performance. The seven-lens optical system produced a PSF where 85% of the spot energy was concentrated in a circle with a diameter of 20 μm**.** This indicates that the system is able to focus the light very well, with very little light spilling into the surrounding area (low aberrations). This results in a high-precision image suitable for accurate measurements of star positions.

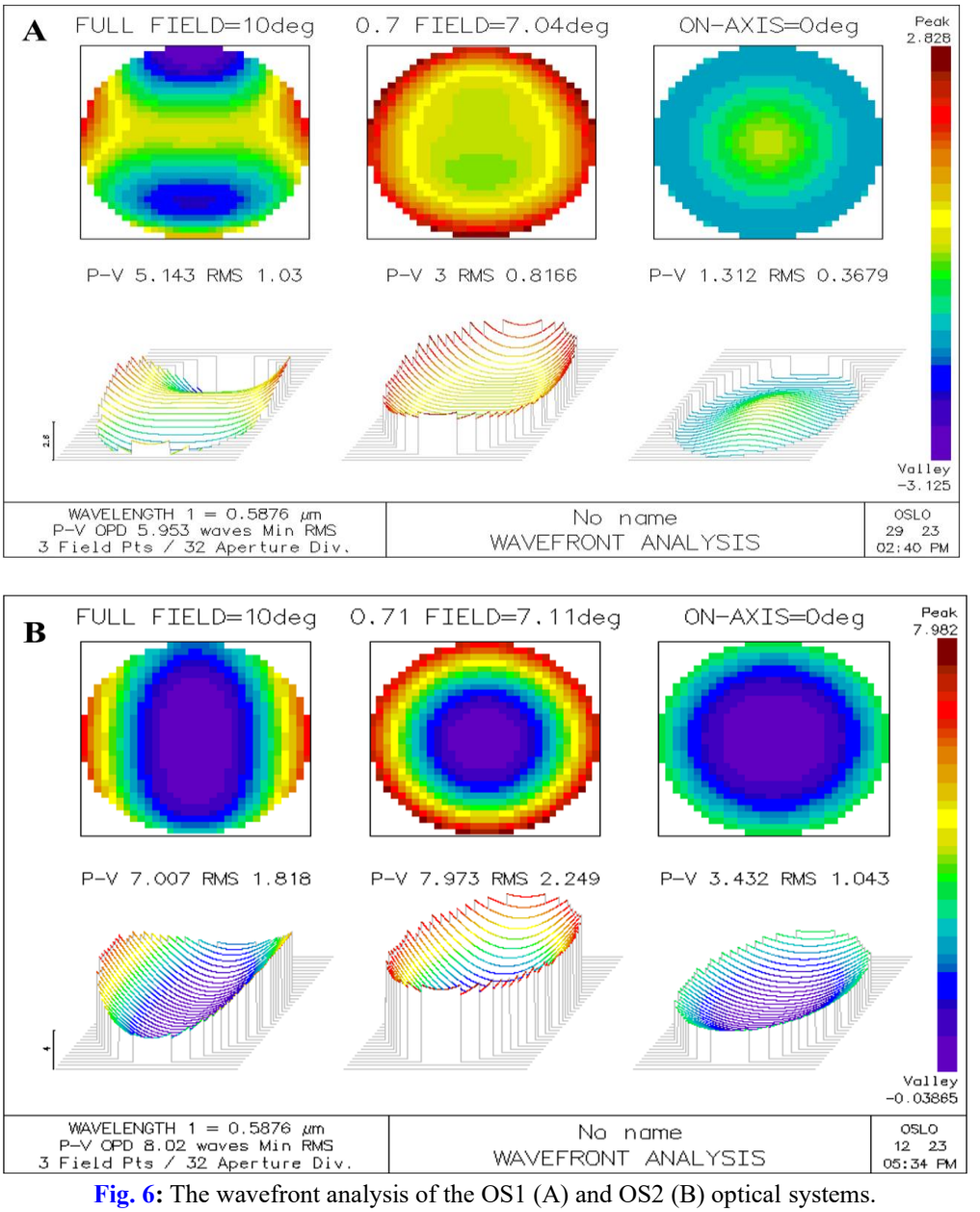

Fig. 6: The wavefront analysis of the OS1 (A) and OS2 (B) optical systems.

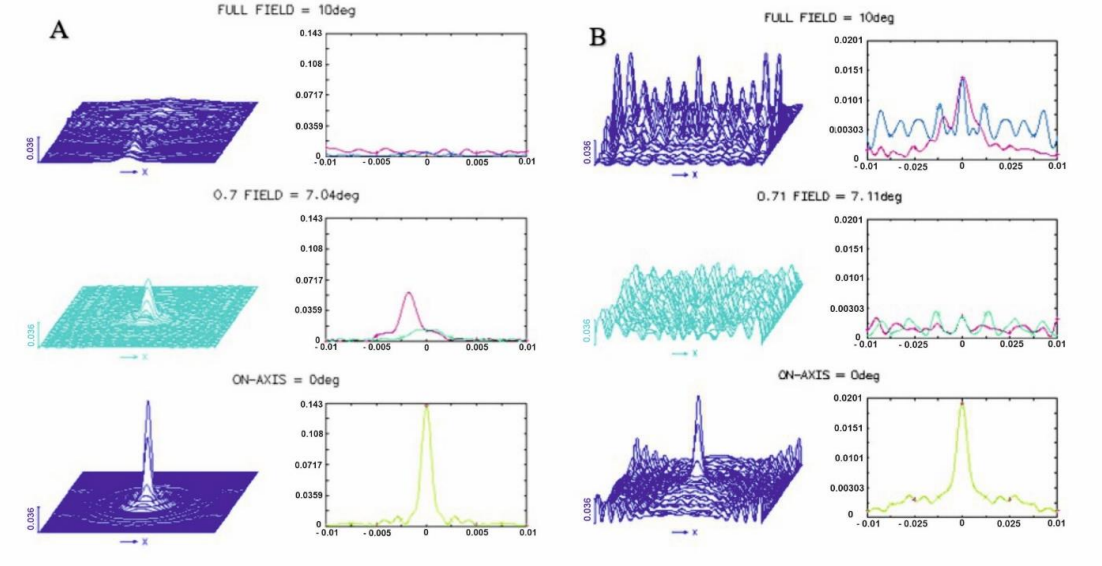

Fig. 7: The analysis of the PSF for OS1 (A) and OS2 (B) optical systems in the field center, 7° and 10° off-axis.

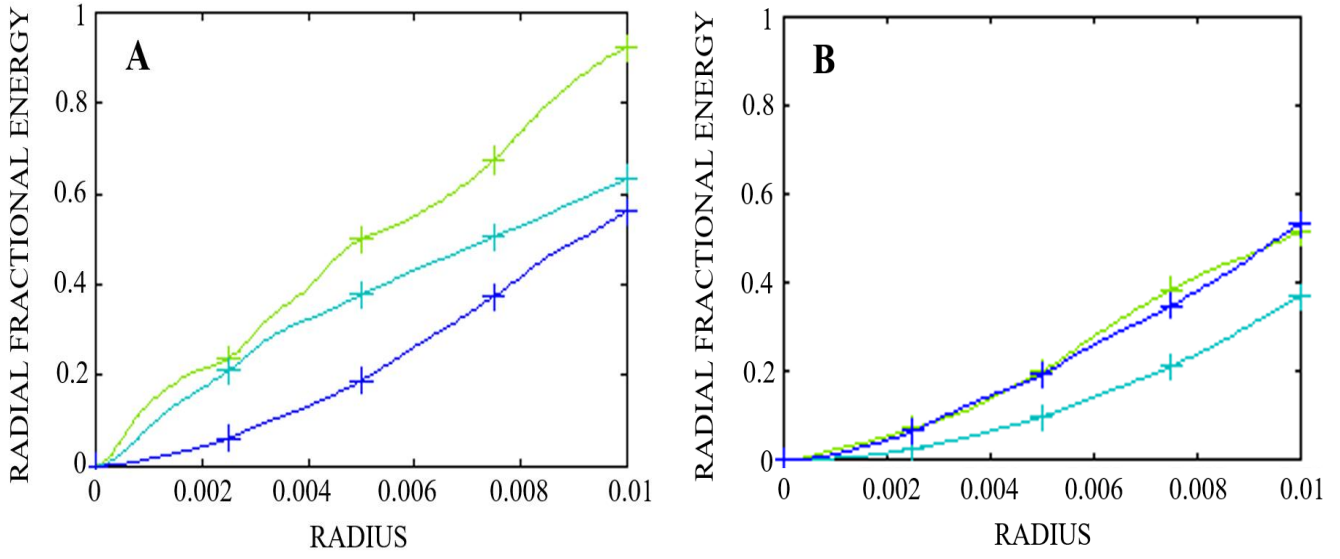

Fig. 8: The radial fractional energies of the OS1 (A) and OS2 (B) optical systems.

Figure 8 shows that for the OS1 optical system 91%, 64%, 58% of the energy in the field center, 7° and 10° off-axis, respectively are concentrated within a circle with a 0.01 mm radius, which is advantageous for the subsequent sub-pixel centroid localization. And for the OS2 optical system these values are 52%, 38%, 52% in the field center, 7° and 10° off-axis, respectively.

4. Conclusion

This study explored methods for enhancing the accuracy of star sensors by analyzing the requirements for high-quality image capture and developing a model of the star sensor's optical system. Two different optical star sensor configurations with varying entrance pupil positions were examined, and their qualitative characteristics were evaluated. The optimal performance was achieved with a seven-lens optical system featuring spherical surfaces and a diaphragm on the first surface, where the PSF concentrated 85% of the spot energy within a 20 μm diameter circle across all field of view angles. The accuracy of the sensor was assessed through OSLO software simulations for different configurations. The findings of this research have significant implications for improving the precision of star sensors, particularly in applications such as spacecraft navigation and astronomical observations, where precise image capture and processing are essential. Furthermore, the approach outlined offers a solid framework for advancing the design of optical systems, providing valuable insights for enhancing sensor performance in various configurations.

Acknowledgements

This research has been funded by the Science Committee of the Ministry of Science and Higher Education of the Republic of Kazakhstan Grant No. AP23487878 Development of GNSS consumer equipment that provides high-accuracy positioning in real time and a posteriori mode.

Conflict of Interest

There is no conflict of interest.

Supporting Information

Not applicable.

References

[1] X. Wang, R. Zheng, Y. Wu, J. Sun, J. Zhong, L. Wang, M. Wang, Study on the method of precision adjustment of star sensor, *Nanotechnology and Precision Engineering*, 2018, **1**, 248-257, doi: 10.1016/j.npe.2018.12.001.

[2] B. Karibayev, N. Meirambekuly, T. Namazbayev, B. Kozhakhmetova, K. Chizhimbayeva, A. Kulakayeva, The possibilities of using fractal antennas in modern wireless communication technologies, 2023 IEEE International Conference on Smart Information Systems and Technologies, Astana, Kazakhstan, May 4-6, 2023.

[3] M. A. A. Fialho, D. Mortari, Theoretical limits of star sensor accuracy, *Sensors*, 2019, **19**, 5355, doi: 10.3390/s19245355.

[4] B. Karibayev, N. Meirambekuly, T. Namazbayev, A. Temirbayev, E. Kadylbekkyzy, A. Yessentaeva, S band TT&C antennas integrated with optical camera system for nanosatellites, 2022 International Conference on Electrical, Computer and Energy Technologies, Prague, Czech Republic, July 20-22, 2022.

[5] Q. Y. Wang, K. Liu, Z. Sun, M. Zhang, Research into the high-precision marine integrated navigation method using INS and star sensors based on time series forecasting BPNN, *Optik*, 2018, **172**, 494-508, doi: 10.1016/j.ijleo.2018.06.007.

[6] M. Z. B. Chowdhury, M. T. Islam, A. Alzamil, M. S. Soliman, M. Samsuzzaman, A tunable star-shaped highly sensitive microwave sensor for solid and liquid sensing, *Alexandria Engineering Journal*, 2024, **86**, 644-662, doi: 10.1016/j.aej.2023.12.001.

[7] N. Meirambekuly, B. A. Karibayev, T. A. Namazbayev, G. A. E. Ibrayev, S. O. Orynbassar, S. A. Ivanovich, A. A. Temirbayev, A high gain deployable L/S band conical helix antenna integrated

with optical system for earth observation CubeSats, *IEEE Access*, 2023, **11**, 23097-23106, doi: 10.1109/ACCESS.2023.3253556.
[8] H. Lei, B. Li, Q. Wei, Y. Yue, X. Ding, K. Liang, L. Chen, H. Yang, W. Zhang, X. Hu, Inertial information based star detection for airborne star sensor, *Optics & Laser Technology*, 2023, **162**, 109325, doi: 10.1016/j.optlastec.2023.109325.
[9] J. Feng, H.-C. Wang, Y.-H. Cui, Y.-D. Li, Q. Guo, L. Wen, J. Fu, Effects of gamma radiation on the performance of star sensors for star map recognition, *Radiation Physics and Chemistry*, 2023, **203**, 110607, doi: 10.1016/j.radphyschem.2022.110607.
[10] N. Meirambekuly, A. A. Temirbayev, Z. Z. Zhanabaev, B. A. Karibayev, T. A. Namazbayev, B. A. Khaniyev, A. K. Khaniyeva, Dual-band optical imaging system-integrated patch antenna based on anisotropic fractal for earth-observation CubeSats, *Ain Shams Engineering Journal*, 2022, **13**, 101560, doi: 10.1016/j.asej.2021.07.010.
[11] A. Shtofenmakher, H. Balakrishnan, Effects of phase angle and sensor properties on on-orbit debris detection using commercial star trackers, *Acta Astronautica*, 2024, **221**, 318-330, doi: 10.1016/j.actaastro.2024.05.028.
[12] S. Steven, J. Bentley, A. Dubra, Design of two spherical mirror unobscured relay telescopes using nodal aberration theory, *Optics Express*, 2019, **27**, 11205-11226, doi: 10.1364/OE.27.011205.
[13] Z. Mu, J. Wang, X. He, Z. Wei, J. He, L. Zhang, Y. Lv, D. He, Restoration method of a blurred star image for a star sensor under dynamic conditions, *Sensors*, 2019, **19**, 4127, doi: 10.3390/s19194127.
[14] I. Remissa, H. Jabri, Y. Hairch, K. Toshtay, M. Atamanov, S. Azat, R. Amrousse, Propulsion systems, propellants, green propulsion subsystems and their applications: a review, *Eurasian Chemico-Technological Journal*, 2023, **25**, 3-19, doi: 10.18321/ectj1491.
[15] K. Alipbayev, K. Saurova, Two basic systems of Maxwell's equations in a rotating frame, *Mechanics of Gyroscopic Systems*, 2022, **44**, 5-12, doi: 10.20535/0203-3771.
[16] Y. Nurgizat, A.-A. Ayazbay, D. Galayko, G. Balbayev, K. Alipbayev, Low-cost orientation determination system for CubeSat based solely on solar and magnetic sensors, *Sensors*, 2023, **23**, 6388, doi: 10.3390/s23146388.
[17] I. Kurmanbayeva, A. Mentbayeva, A. Nurpeissova, Z. Bakenov, Advanced battery materials research at nazarbayev university: review, *Eurasian Chemico-Technological Journal*, 2021, **23**, 199, doi: 10.18321/ectj1103.
[18] L. Jannin, L. Felicetti, Calibration and testing strategies to correct atmospheric effects on star tracking algorithms, *Astronomy and Computing*, 2024, **46**, 100794, doi: 10.1016/j.ascom.2024.100794.
[19] D. Spiller, F. Curti, A geometrical approach for the angular velocity determination using a star sensor, *Acta Astronautica*, 2022, **196**, 414-431, doi: 10.1016/j.actaastro.2020.11.043.
[20] T. Sun, F. Xing, X. Wang, Z. You, D. Chu, An accuracy measurement method for star trackers based on direct astronomic observation, *Scientific Reports*, 2016, **6**, 22593, doi: 10.1038/srep22593.
[21] X. Wang, X. Chen, Z. Li, J. Zhu, An optical system of star sensors with accuracy performance varying with the field of view, *Sensors*, 2023, **23**, 8663, doi: 10.3390/s23218663.
[22] J. Lu, C. Lei, Y. Yang, A dynamic precision evaluation method for the star sensor in the stellar-inertial navigation system, *Scientific Reports*, 2017, **7**, 4356, doi: 10.1038/s41598-017-04061-5.